Journal of Molecular Structure 936 (2009) 46–55

Contents lists available at ScienceDirect

Journal of Molecular Structure

journal homepage: www.elsevier.com/locate/molstruc

5-Benzyl-4-[3-(1H-imidazol-1-yl)propyl]- 2H-1,2,4-triazol-3(4H)-ones: Synthesis, spectroscopic characterization, crystal structure and a comparison of theoretical and experimental IR results by DFT calculations

Yasemin Ünver [a,*], Kemal Sancak [a], Hasan Tanak [c], İsmail Değirmencioğlu [a], Esra Düğdü [a], Mustafa Er [b], Şamil Işık [c]

[a] Department of Chemistry, Faculty of Arts and Sciences, Karadeniz Technical University, 61080 Trabzon, Turkey
[b] Department of Chemistry, Karabük University, 78200 Karabük, Turkey
[c] Department of Physics, Ondokuz Mayıs University, Samsun, Turkey

ARTICLE INFO

Article history:
Received 16 June 2009
Received in revised form 15 July 2009
Accepted 16 July 2009
Available online 12 August 2009

Keywords:
1,2,4-Triazoles
Imidazol
IR
DFT calculations
UV–vis
X-ray crystallography

ABSTRACT

The synthesis and structural properties of novel compounds, 5-Benzyl- 4-[3-(1H-imidazol-1-yl)propyl]-2H-1,2,4-triazol-3(4H)-ones **(3a–c)** have been described. These products were obtained by the reaction of ethyl 2-[1-ethoxy-2-(phenyl or substituted phenyl)ethylidene]hydrazinecarboxylates **(1)** and *N*-(3-aminopropyl)imidazol **(2)**. The structures of compounds **3a–c** have been inferred through UV–vis, IR, $^{1}H/^{13}C$ NMR, mass spectrometry, elemental analyses, and X-ray crystallography. DFT level 6-31G*(d,p) calculations provided structural information and IR data that were in good agreement with experimental results for compound **3a**. Additionally, the electronic structure of compound **3a** has been studied by DFT level 6-31G*(d,p) calculations using the X-ray data.

1. Introduction

The 1,2,4-triazoles posses important pharmacological properties such as antifungal and antiviral activities. Examples of such compounds bearing the 1,2,4-triazole residues are fluconazol [1], the powerful azole antifungal agent as well as the potent antiviral *N*-nucleoside ribavirin [2]. Furthermore, various 1,2,4-triazole derivatives have been reported as fungicidal [3], insecticidal [4], antimicrobial compounds [5], and some showed antitumor activity [6], or are anticonvulsants [7], antidepressants [8], and plant growth regulator anticoagulants [9]. It was reported that compounds having triazole moieties such as vorozole, anastrozole and letrozole appear to be very effective aromatase inhibitors, which are very useful for preventing breast cancer [10–12]. It is known that 1,2,4-triazol moieties interact strongly with heme iron, and aromatic substituents on the triazoles are very effective for interacting with the active site of aromatase [13].

Since the first report on the air and H_2O stable ionic liquids in 1992 [14], versatile ionic liquids have been investigated [15–25]. Recently, the interest in triazol and imidazol heterocyclic system has widened as it is a precursor to a class of compounds called 'room temperature ionic liquids' [26]. Ionic liquids have high ion content, high ionic conductivity, low viscosity, nonvolatility, flame resistance, and other surprising properties as a polar liquid, and have therefore been investigated as a novel ion conductive matrix [16–33], as well as reaction solvent [32] and a 'green solvent' [33,34].

Ionic liquids, of which imidazolium salts are most widely used, have gained initial notice of synthetic chemists as environmentally friendly organic solvents, and continue to hold their attention as reaction catalysts or promoters [35]. Additionally, They have the ability to dissolve an enormous range of inorganic, organic, and polymeric materials at very high concentrations, are noncorrosive, and have low viscosities and no significant vapor pressures [36,37].

In view of these facts, the aim of the present study is to synthesize the triazole-3 one compounds containing imidazol which are fundamental compounds in the preparation of ionic liquids and used as a antimicrobial substance.

* Corresponding author. Tel.: +90 462 377 24 85; fax: +90 462 325 31 95.
E-mail address: yasemincan@ktu.edu.tr (Y. Ünver).

0022-2860/$ - see front matter © 2009 Elsevier B.V. All rights reserved.
doi:10.1016/j.molstruc.2009.07.045

2. Experimental

2.1. Physical measurements

^{1}H NMR and ^{13}C NMR spectra were recorded on a *Varian XL-200* NMR spectrophotometer in (D_6) DMSO. IR spectra were recorded on a *Perkin–Elmer Spectrum one FT-IR* spectrometer (resolution 4) in KBr pellets. The MS spectra were measured with an *Micromass Quattro LC/ULTIMA LC-MS/MS* spectrometer with EtOH as solvent. The experiment was performed in the positive ion mode. Elemental analyses were performed on a *Hewlett–Packard 185 CHN analyzer*. UV/vis spectra were recorded by means of a *Unicam UV2–100* spectrophotometer. M.p. were measured on an electrothermal apparatus and are uncorrected. The molecular data were collected on an *Stoe IPDS II* [38] diffractometer using the Mo Kα radiation at room temperature. For the compounds **3a–c** data collection: X-AREA [38]; cell refinement: X-AREA; data reduction: X-RED32 [38]; program used to solve structure: SHELXS97 [39]; program used to refine structure: SHELXL97 [39]; molecular figures: ORTEP III [40]; publication software: WinGX [41] and PARST [42]. The structures were solved by direct methods with SHELXS-97 and refined by full-matrix least-squares procedures on F^2, using the program SHELXL-97 computer program belonging to the WinGX software package.

2.2. Materials

The compound **(1)** was prepared as described by Ikizler and Sancak [43]. All reactions were carried out under an atmosphere of dry, O_2-free N_2, using standart Schlenk techniques. The used solvents (acetone, and petroleum ether) were either of analytical grade or bulk solvents distilled before use.

2.3. Preparation of compounds (*3a-c*)

Ethyl 2-[1-ethoxy-2-(phenyl or substituted phenyl)ethylidene]hydrazine carboxylates (**1**) (10 mmol) together with N-(3-aminopropyl)imidazole (**2**) (1.25 g, 10 mmol) were heated without solvent in a sealed tube for 2 h at 160 °C. Then, the mixture was cooled to r.t. and a solid formed. The crude product was recrystallized using acetone/petroleum ether (1:2) to afford the desired compound.

2.3.1. 5-Benzyl-4-[3-(1H-imidazol-1-yl)propyl]-2H-1,2,4-triazol-3(4H)-one (*3a*)

Yield: 221 mg (72%). Colorless crystals. M.p. 161°–162°.

Anal. calc. for $C_{15}H_{17}N_5O$: C, 63.59; H, 6.06; N, 24.72. Found: C, 63.62; H, 6.05; N, 24.73.

IR (KBr,cm^{-1}): 1462 (C=N); 1720 (C=O).

^{1}H NMR (200 MHz, $DMSO_{d6}$): 1.60–1.68 (m, 2H, H—C(12)); 3.39 (t, 4H, *J* = 3.6, H—C(7) + H—C(13)); 3.87 (t, 2H, *J* = 3.4, H—C(11)); 6.98 (s, 1H, H—C(14)); 7.10 (s, 1H, H—C(15)); 7.23 (s, 2H, H—C(2)) + H—C(6)); 7.28 (s, 2H, H—C(3) + H—C(5)); 7.32 (s, 1H, H—C(4)); 7.58 (s, 1H, H—C(16)); 11.59 (s,1H, H—C(9)).

^{13}C NMR (200 MHz, $DMSO_{d6}$): 29.94 (C(12); 32.81 (C(7)); 38.72 (C(13)); 44.09 (C(11)); 118.61 (C(14)); 129.71 (C(15)); 137.06(C(16)); 127.75 (C(2) + (C(6)); 128.41 (C(3) + (C(5)); 129.23 (C(4)), 134.27 (C(1)); 146.47 (C(8)); 156.02 (C(10)).

MS(ESI-m/z): 283.99 [M]$^+$.

2.3.2. 4-(3-(1H-imidazol-1-yl)propyl)-5-(3,4-dimethoxybenzyl)-2H-1,2,4-triazol-3(4H)-one (*3b*)

Yield: 167 mg (73%). Colorless crystals. M.p. 167–168 °C Anal. calc. for $C_{17}H_{21}N_5O_3$: C, 59.46; H, 6.16; N, 20.41. Found: C, 59.43; H, 6.15; N, 20.45.

IR (KBr, cm^{-1}): 1580 (C=N); 1714 (C=O).

^{1}H NMR (200 MHz, $DMSO_{d6}$): 1.70–1.84 (m, 2H, H—C(12)); 3.48 (t, 2H, *J* = 3.6, H—C(13)); 3.76 (s, 2H, H—C(7)); 3.87 (t, 8H, *J* = 6.7, H—C(11) + H—C(17)); 6.64–6.66 (m, 2H, H—C(5) + H—C(6)); 6.77–6.83 (m, 2H, H—C(2) + H—C(14)); 7.09 (s, 1H, H—C(15)); 7.47 (s, 1H, H—C(16)); 11.56 (s, 1H, H—C(9)).

^{13}C NMR (200 MHz, $DMSO_{d6}$): 29.20 (C(12); 39.46 (C(13)); 42.00 (C(7)); 49.27 (C(11)); 55.22 (C(17)); 120.64 (C(14)); 128.19 (C(15)); 136.72 (C(16)); 111.69 (C(2)); 112.22 (C(5)); 120.40 (C(6)); 130.14 (C(1)); 146.44 (C(4)); 147.39 (C(3)); 145.86 (C(8)); 156.90 (C(10)).

MS(ESI-m/z): 344.20 [M]$^+$.

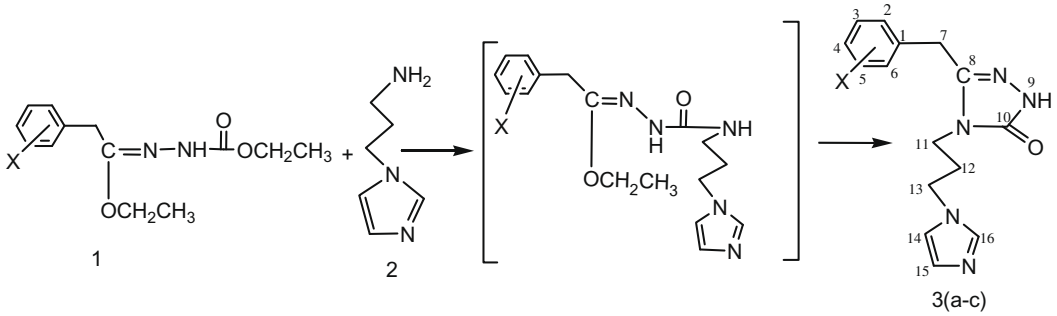

3	X
a	H
b	3,4-^{17}MeO
c	4-NO2

Scheme 1. Synthetic route to target compounds **3(a–c)**.

*2.3.3. 4-(3-(1H-imidazol-1-yl)propyl)-5-(4-nitrobenzyl)-2H-1,2,4-triazol-3(4H)-one (**3c**).*

Yield: 156 mg (69%). Colorless crystals. M.p. 169–170 °C.

Anal. calc. for $C_{15}H_{16}N_6O_3$: C, 54.87; H, 4.91; N, 25.60. Found: C, 54.86; H, 4.89; N, 25.64.

IR (KBr, cm^{-1}): 1584 (C=N); 1697 (C=O); 1355,1520 (NO_2).

^1H NMR (200 MHz, $DMSO_{d6}$): 1.85–1.92 (m, 2H, H—C(12)); 3.33 (s, 2H, H—C(7)); 3.48 (t, 2H, *J* = 3.6, H—C(13)); 3.90 (t, 2H, *J* = 3.4, H—C(11)); 6.94 (s, 1H, H—C(14)); 7.06 (s, 1H, H—C(15)); 7.46 (d, A–A', 2H, *J* = 8.8, H—C(2) + H—C(6)); 7.60 (s, 1H, H—C(16)); 8.15 (d, B–B', 2H, *J* = 8.8, H—C(3) + H—C(5)) ; 11.60 (s, 1H, H—C(9)).

^{13}C NMR (200 MHz, $DMSO_{d6}$): 30.01 (C(12); 38.61 (C(13)); 42.16 (C(7)); 46.25 (C(11)); 119.76 (C(14));129.73 (C(15)); 137.35 (C(16)); 123.80 (C(2) + (C(6)); 129.80 (C(3) + (C(5)); 143.78 (C(1)); 144.90 (C(4)); 144.87 (C(8)); 155.89 (C(10)).

MS(ESI-m/z): 329.10 $[M]^+$.

Table 1
Observed and calculated frequencies (cm^{-1}), calculated IR intensities (km/mol), and probable assignment of normal modes for compound **3a.**

Observed	Calculated/6–31G*(d,p)	Intensities	Assignment
3417(m)	3501	21.37	$\upsilon_{s(NH)}$
3080(ms)	3097	44	$\upsilon_{as(CH)}$
3014(ms)	3061	40.88	$\upsilon_{s(CH)}$
2996(ms)	2974	40.77	$\upsilon_{as(CH)}$
2810(ms)	2922	42.84	$\upsilon_{s(CH)}$
1720(vs)	1713	153.19	$\upsilon_{C=O}$
1636(m)	1612	50.14	$\upsilon_{C=C}$
1580(ms)	1568	38.01	$\upsilon_{as(ring)}$
1522(m)	1522	93.56	$\upsilon_{s(ring)} + \delta_{NH}$
1510(m)	1510	31.98	$\delta_{s(CHimidazole/triazole)} + \delta_{s(CH2)}$
1462(ms)	1454	53.98	$r_{CHimidazole} + r_{CH2} + \delta_{C=Nimidazole/C\text{-}imidazole}$
1440(m)	1437	35.03	$\delta_{CHimidazole/CHbenzene} + r_{CH2}$
1431(m)	1430	34.98	$\delta_{s(CH2)}$
1420(m)	1416	12.21	$\delta_{s(CH2)}$
1394(mw)	1398	27.11	$r_{ring} + r_{CH2}$
1373(w)	1372	21.91	$r_{ring} + r_{CH2} + \delta_{NH}$
1343(mw)	1339	25.39	$\delta_{CN} + r_{ring} + r_{CH2}$
1325(mw)	1312	9.66	$r_{CHimidazole/triazole} + \delta_{C\text{-}Nimidazole} + \delta_{s(CH2)}$
1285(mw)	1283	92.12	$r_{CHimidazole/triazole} + \delta_{s(CH2)} + \delta_{NH} + \delta_{NHCO}$
1255(m)	1267	32.56	$\delta_{s(ring)} + \delta_{s(CH2)}$
1230(ms)	1231	40.97	$\delta_{s(ring)} + \delta_{s(CH=Nimidazole)}$
1215(mw)	1212	23	$\delta_{s(ring)}$
1183(mw)	1190	3.16	$\delta_{s(CHimidazole/triazole)} + \delta_{s(CH2)}$
1145(w)	1137	4.09	$\delta_{s(ring)} + \delta_{NH}$
1108(m)	1111	31.05	$\delta_{s(CHimidazole/triazole)} + \delta_{s(CH2)} + r_{ring}$
1079(ms)	1078	41	$r_{ring} + r_{CHimidazole/triazole}$
1059(mw)	1069	17.74	$r_{CHimidazole/triazole}$
1040(mw)	1045	19.99	$\delta_{s(ring)} + \delta_{s(CH2)}$
1027(w)	1019	5.91	γ_{ring}
998(m)	990	31.92	γ_{ring}
919(m)	919	4.26	$r_{CHimidazole/triazole} + r_{CH2}$
876(w)	889	6.22	$\delta_{s(CHimidazole/triazole)} + \delta_{s(CH2)} + \gamma_{ring}$
850(mw)	847	33	$\gamma_{ring} + \delta_{s(CHimidazole)}$
829(ms)	823	86.94	$\delta_{s(CH2)} + \upsilon_{C=O} + \delta_{NH}$
750(ms)	758	40	$\delta_{ring\text{-}mono\ subs.} + \gamma_{CHimidazole}$
728(ms)	729	22.43	$\delta_{s(CH2)} + \gamma_{ring\text{-}mono\ subs.} + \upsilon_{C=O} + \delta_{NH}$
662(m)	667	7.71	$\gamma_{ring} + \gamma_{CHimidazole/triazole} + \delta_{NH}$
630(mw)	632	5.44	$\gamma_{CHimidazole/triazole} + \delta_{s(CH2)}$
605(mw)	607	1.11	$\gamma_{CHimidazole/triazole} + \delta_{s(CH2)} + \delta_{NH}$
558(w)	560	0.65	$\gamma_{ring} + \delta_{s(CH2)} + \delta_{NH}$
545(w)	520	12.92	$\gamma_{ring} + \delta_{s(CH2)} + \delta_{NH}$
482(w)	472	1.25	$\gamma_{ring} + \delta_{s(CH2)}$
461(w)	461	3.21	$\gamma_{ring} + \delta_{s(CH2)}$

Vibrational modes: υ, stretching; δ, in-plane deformation; δ_s, scissoring; *r*, rocking; γ, out-of-plane deformation. Superscript: s, symmetric; as, asymmetric; ring, benzene; w, weak; m, medium; ms, medium strong; mw, medium weak.

3. Results and discussion

The synthesis of 5-Benzyl-4-[3-(1H-imidazol-1-yl)propyl]-2H-1,2,4-triazol-3(4H)-ones (**3**) was obtained by the reaction of compounds **(1)** and compound (**2**) (Scheme 1). Analytical and spectroscopic data of the products **3a-c** confirmed the success of the cyclization reaction.

The IR data indicated the formation of compounds **3a–c** by the disappearance of $COCH_2$ (esteric) band of **(1)** at 1247 cm^{-1}, and the new band at 1697–1714 cm^{-1} belonging to the triazole C=O. In the IR spectrum of compound **3c**, the NO_2 group was recorded at 1355 and 1520 cm^{-1}. The EI–MS of compounds **3a–c** confirmed the proposed structures with a molecular ion peak at *m/z* = 283.99, 344.20, and 329.10, respectively.

In the ^1H NMR spectra, the existence of **3a–c** was revealed by the disappearance of form of the ester CH_2O groups (4.18–4.24 ppm) in the precursor **(1)** after the cyclization and the appearance of a new peak at 11.56–11.60 ppm integrating for one H-atom (exchangeable with D_2O) belonging to H—N(10) [44].

The $H_2C(12)$ groups of the propyl residue attached to the triazol and imidazol rings resonate as a multiplet between 1.60–1.92 ppm, while $H_2C(13)$, linked to the imidazol ring, was recorded at 3.39–3.48 ppm as a triplet, and H—C(11) linked to the triazol ring was observed at 3.87–3.90 ppm as triplet.

Coupling constants *J* between the imidazol H—C(14) and H—C(15) were often very small or not observable in DMSO but sometimes are visible in $D_2O/CDCl_3$ [45]. In (D_6) DMSO, H—C(15) and H—C(14) of the imidazol ring of **3a–c** resonate as two singlets at 6.94–6.98 and 7.06–7.10 ppm, respectively. A singlet at 7.47–7.60 ppm was observed for H—C(16).

More detailed information about the structure of compounds **3a–c** was provided by the ^{13}C NMR spectra. The CH_2 groups C(7), C(11), C(12) and C(13) with aliphatic character showed resonances at 32.81–42.16, 44.09–46.25, 29.20–30.01, and 38.46–38.71 ppm, respectively. The signals for the triazole C(8) and the C=O group C(10) are found at 144.87–146.47 and 155.89–156.02 ppm, respectively. The other aromatic C-atoms bearing H-atoms (C(2), C(3), C(4), C(5), C(6), C(14), C(15), C (16)) are observed at 111.69–123.80, 129.80–147.39, 129.23–146.44, 112.22–144.90, 120.40–127.75, 118.61–119.76, 128.19–129.73, 136.72–137.35 ppm, respectively. Finally, C(1) absorbs at 130.14–143.78 ppm.

4. Method of calculations

*4.1. Comparison of the theoretical and experimental Infrared spectra of compound (**3a**)*

In order to construct of ligand molecule, the geometrical parameters of ligand **3a** were taken from X-ray structure data. The molecular structure of ligand in the ground state was optimized by density functional using Becke's three-parameter hybrid method (B3) with the Lee, Yang and Parr correlation functional methods (LYP) with the Standard 6-31G*(d,p) basis set [46,47]. The optimized structural parameters were used in the vibrational frequency calculations at DFT level to characterize all stationary points as minima. 6-31G*(d,p) basis set was used for all elements. All calculations were performed with the Gaussian 03W program package [48]. In calculations, tight converge criteria was used. By allowing that all the parameters could relax, all the calculations converged to optimized geometries, which corresponded to true energy minima. The frequency values computed at this level contain known systematic errors [50]. Therefore, we have used the scaling factor value of 0.9614 for B3LYP [51]. The vibrational assignments inferred in Table 1, via the Gaussview program, have been severally checked and than combined. By combining the results of the Gaussview

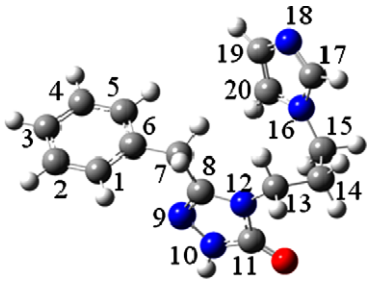

Fig. 1. Calculated molecular structure of 5-Benzyl- 4-[3-(1H-imidazol-1-yl)propyl]-2H-1,2,4-triazol-3(4H)-one (**3a**) with atomic numbering.

program with symmetry considerations, vibrational frequency assignments were made with accuracy. There is always some ambiguity in defining internal coordination. However, the described coordinate generates the studied set and matches quite well with the motions observed using the Gaussview program. On the basis of the optimized ground state structure, the spectroscopic properties and UV–vis absorption calculations in vacuum have been carried out by using the time-dependent density functional theory (TD-DFT) at B3LYP level, providing an accurate description of UV–vis transitions of ligand system.

4.2. Molecular geometry

The calculated vibrational spectrum has no imaginary frequency, which indicates that the optimized geometry is located at the minimum point on the potential energy surface. The calculations were performed at the point group C(1). The optimized molecular structure turns out to be very close to the X-ray diffraction structure of ligand molecule. For comparison, we present the main geometric parameters of **3a**, obtained both by X-ray diffraction and by calculation at the DFT/6-31G*(d,p)-B3LYP level in Table 1. The correlation coefficients of the experimental and theoretical geometric parameters are calculated to be 0.9614, 0.9545, and 0.9986 for the bond lengths, bond angles, and torsional angles, respectively. As shown in Table 1, the theoretical values are in good agreement with the experimental measurements [49,52–54].

4.3. Vibrational spectra

4.3.1. NH and CH stretching modes

Most organic compounds have CH bonds; a useful rule is that absorption in the 2850–3000 cm^{-1} is due to sp^3–CH stretching whereas absorption above 3000 cm^{-1} is from sp^2 CH stretching. Also the assignments of the CH_2 stretching bands are always ambiguous since they are coupled with the overtone and combination band of CH_2 bending at around 1450 cm^{-1}. In this work, a major harmony of theoretical values with that of experimental evaluations was found in the symmetric and asymmetric stretching vibrations of aromatic CH and CH_2 moiety. Four bands in the region 3100–2810 cm^{-1} were observed in the spectrum. These assignments are also supported by *Silverstein* and other [49,55]. The first two bands are depolarized and the latter two bands are strong and polarized in the spectrum, therefore, we assigned these bands to the out-of-plane and in-plane asymmetric and symmetric —CH_2 stretching modes, respectively. In addition, in the heterocyclic compounds, υ_{N-H} vibration occurs in the region 3500–3000 cm^{-1}. The IR band appearing at 3417 cm^{-1} is assigned to the υ_{N-H} stretching mode of vibrations. This vibration mode calculated at 3501 cm^{-1} for DFT method. The difference between

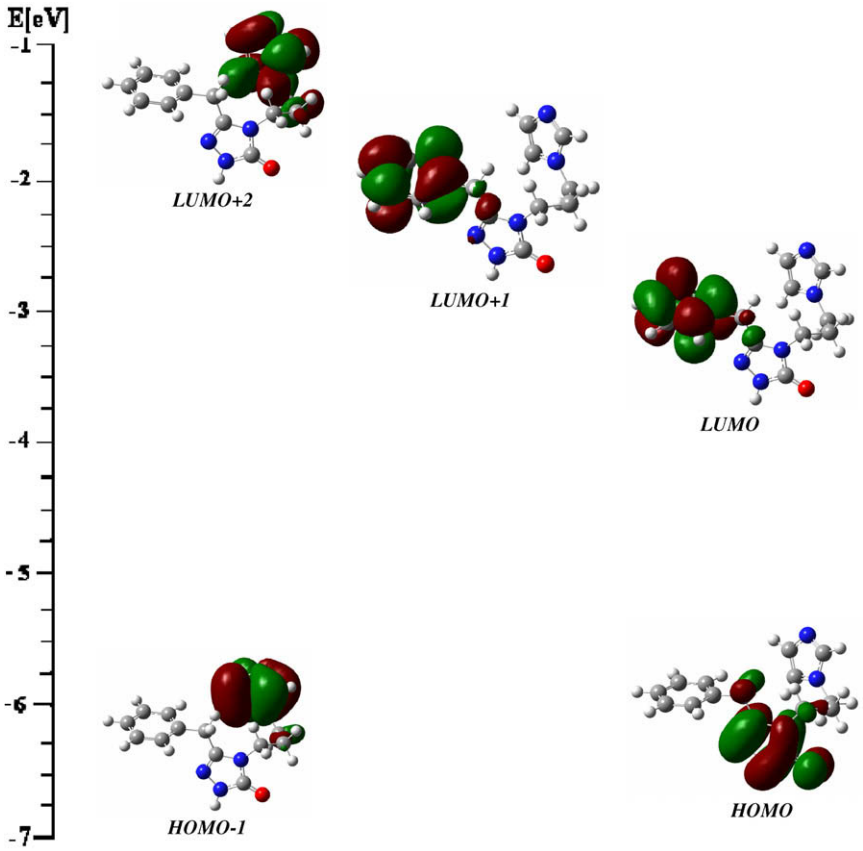

Fig. 2. Frontier orbitals for **3a.**

Table 2
Experimental λ (nm), selected/calculated TD-DFT singlet energies, MO transitions, oscillator strengths.

Orbital (transitions)	MO coefficiens	Oscillator	Assignment	λ_{exp} (nm)	λ_{calc} (nm)	Bond type
HOMO → LUMO (88 → 89)	0.631	0.4607	$\pi \rightarrow \pi^*$	324	324.1	π(C=C)/(C=O) → π^*(C=C)
HOMO → LUMO + 1 (88 → 90)	0.393	0.0736	$\pi \rightarrow \pi^*$	309	319.5	π(C=C)/(C=O) → π^*(C=C) and
HOMO−1 → LUMO (87 → 89)	0.439					π(C=C)/(C=N) → π^*(C=C)
HOMO → LUMO + 2 (88 → 92)	0.349	0.0872	$\pi \rightarrow \pi^*$/	295	299.2	π(C=C)/(C=O) → π^*(C=C) and
HOMO−1 → LUMO + 1 (87 → 90)	0.379		nb → π^*			π(C=C)/(C=N) + nb (N16) → π^*(C=C) and
HOMO−1 → LUMO + 2 (87 → 91)	0.397					π(C=C)/(C=N) + nb (O) → π^*(C=C)/(C=N)
HOMO−1 → LUMO + 1 (87 → 90)	0.671	0.114	$\pi \rightarrow \pi^*$/ nb → π^*	285	287.9	π(C=C)/(C=N) + nb (N16) → π^*(C=C)
HOMO−1 → LUMO + 2 (87 → 91)	0.317	0.0845	$\pi \rightarrow \pi^*$ / nb → π^*	255	256.1	π(C=C)/(C=N) + nb (O) → π^*(C=C)/(C=N)
HOMO−1 → LUMO + 2 (87 → 91)	0.441	0.639	$\pi \rightarrow \pi^*$	239	243	π(C=C)/(C=N) → π^*(C=C)/(C=N)
HOMO → LUMO + 2 (88 → 91)	0.576	0.091	$\pi \rightarrow \pi^*$	236	236.7	π(C=C)/(C=O) → π^*(C=C) and
HOMO−1 → LUMO + 2 (87 → 91)	0.337					π(C=C)/(C=N) → π^*(C=C)/(C=N)

experimental and calculated υ_{N-H} stretching mode is about 84 cm^{-1}. This striking discrepancy may come from difference between solid and gas phase, but the IR spectrum of **3a** was taken in KBr pellets while the theoretical calculation of molecule was performed in gas phase.

4.3.2. 1700–1000 cm^{-1} region

In this region, the strong stretching vibration of the carbonyl bond contributes to the observed band at 1720 cm^{-1}, corresponding to the frequency predicted to be at 1713 cm^{-1}. The $\upsilon_{C=C}$ stretching vibration was calculated to lie at 1636 cm^{-1}, close to the typical value. The environment atom next to the double bond does not affect the bond strength appreciably.

The calculated intensities $\upsilon_{C=C}$ stretching and $\delta_{s(ring/=CHimidazole/=CHtriazole/-CH2)}$ in-plane bending vibrations are equal while the typical intensities in the spectral correlation tables are weak and strong, respectively [49]. The bands due to the ring(benzene) and $CH_{imidazole/triazole}$ stretching are found in the experimental solid IR spectrum at 1636–1522 cm^{-1} and also the bands at 1510.7–1040.4 cm^{-1} are assigned to the in-plane and out-of-plane ring, methylene and $CH_{imidazole/triazole}$ bending vibrations. The deformation vibrations of $-CH_2$ group (scissoring, wagging, twisting and rocking) contribute to several vibration modes in low frequency region. As seen from Table 1, the bands at 1462.5, 1440.7, 1420.1, 1343.2, 1285.7, 1183.8 cm^{-1} in the FT-IR spectrum corresponds to all deformation $-CH_2$ modes, respectively. The scissoring, wagging, twisting and rocking vibrational modes are distributed in a wide range [49,56]. The identification of υ_{CN} vibrations is a difficult task, since the mixing of vibrations is possible in this region. However, with the help of the animation option of Gauss View 3.0 graphical interface for gaussian programs, the υ_{CN} vibrations are identified and assigned in this study. As a result, the IR bands appearing at 1462.5, 1343.2, 1325.7 and 1230.5 cm^{-1} are assigned to the υ_{CN} vibrations with combination of the $\delta_s/Q_{(=CHimidazole/triazole)}$ and $\delta_{s(ring)}$ for the compound **3a**.

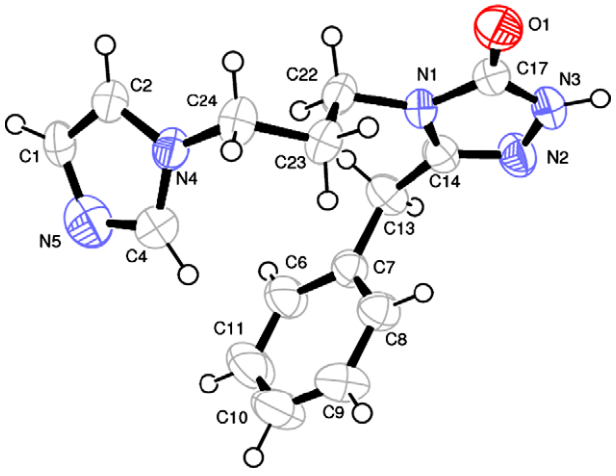

Fig. 3. Ortep III diagram of **3a**.

4.3.3. 1000–400 cm^{-1} region

The medium bands at 998.5, 919.6, 876.8, 850.7, 630.9, 482 and 461 cm^{-1} are assigned to the imidazole and triazole ring deformation (in-plane and out-of-plane) vibrations comparing with the predicted frequencies at 990.9, 919.96, 889.72, 847.15, 632.06, 472.66 and 461.05 cm^{-1}, respectively. The additional ring deformation vibrations with $\delta_{s(CH2)}$, $\delta_{C=O}$ and δ_{NH} are calculated to be at 829.3, 558.3 and 545 cm^{-1} with medium and weak intensities. Two of the ring torsion modes are predicted to be at 758.2 and 729.49 cm^{-1}, and were observed at 750 and 728.5 cm^{-1} in the experimental spectrum. As could not be seen any deformation vibrations below 400 cm^{-1} in the experimental spectrum, calculated deformation vibrations below 400 cm^{-1} were neglected.

*4.4. Theoretical aspects of UV–vis spectrum of compound **3a***

The Experimental UV–vis spectrum of **3a** was measured in chloroform solution, and it was found that the absorption bands maximized at 324, 309, 295, 285, 255, 239 and 236 nm. In order to

Table 3
Crystal and experimental data for compounds **3a–c.**

3a	**3b**	**3c**
Formula: $C_{15}H_{17}N_5O$	Formula: $C_{17}H_{21}N_5O_3$	Formula: $C_{15}H_{16}N_6O_3$
Formula weight: 283.34	Formula weight: 343.39	Formula weight: 328.34
Crystal system: orthorhombic	Crystal system: monoclinic	Crystal system: monoclinic
Space group: $Pna2_1$	Space group: $P2_1/c$	Space group: $P2_1/c$
Z = 4	Z = 4	Z = 4
a = 10.9331(5) Å	a = 16.4386(12)Å	a = 9.0096(5) Å
b = 14.9317(10) Å	b = 6.3326(3) (10)Å	b = 6.6083(2) Å
c = 8.9848(6) Å	c = 17.3148(12)Å	c = 26.8310(15)Å
$\alpha = \beta = \gamma = 90$, and V = 1466.77(15) $Å^3$	β = 105.289(6), and V = 1738.66(19)$Å^3$	β = 102.594(4), and V = 1559.03(13) $Å^3$
No. of reflections used = 9748	No. of reflections used = 9748	No.of reflections used = 9183
$2\theta_{max}$ = 60° Mo Kα	$2\theta_{max}$ = 60° Mo Kα	$2\theta_{max}$ = 60° Mo Kα
R = 0.050	R = 0.050	R = 0.053
$(\Delta/\sigma)_{max}$ = 0.000	$(\Delta/\sigma)_{max}$ = 0.000	$(\Delta/\sigma)_{max}$ = 0.000
$(\Delta/\rho)_{max}$ = 0.346 e$Å^{-3}$	$(\Delta/\rho)_{max}$ = 0.346 e$Å^{-3}$	$(\Delta/\rho)_{max}$ = 0.143 e$Å^{-3}$
$(\Delta/\rho)_{min}$ = −0.297 e$Å^{-3}$	$(\Delta/\rho)_{min}$ = −0.297 e$Å^{-3}$	$(\Delta/\rho)_{min}$ = −0.149 e$Å^{-3}$
F(0 0 0) = 600	F(0 0 0)= 728	F(0 0 0)= 688
μ = 0.086 mm^{-1}	μ = 0.093 mm^{-1}	μ = 0.102 mm^{-1}

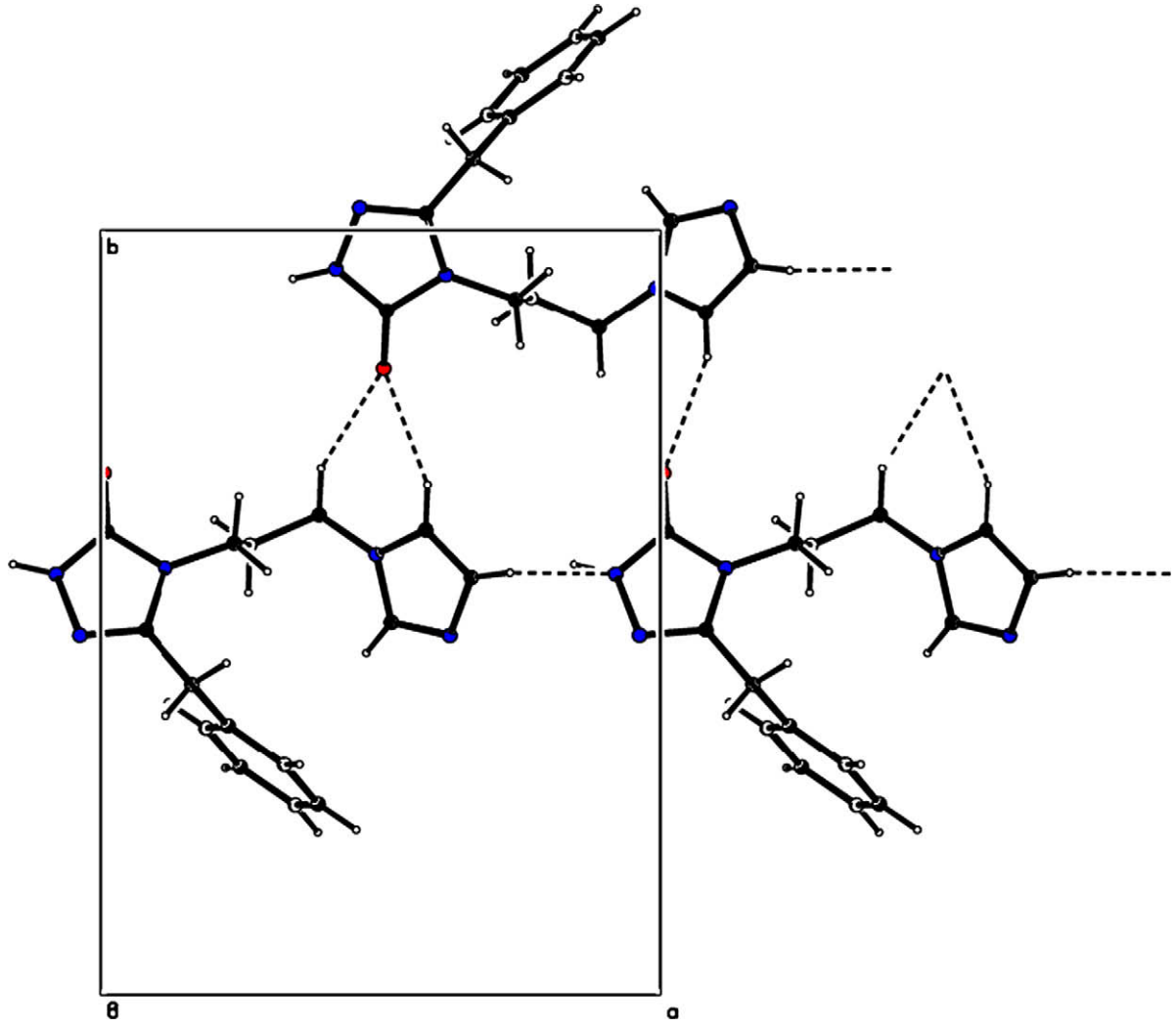

Fig. 4. Packing diagram of **3a.**

understand electronic transitions of **3a**, TD-DFT calculations on electronic absorption spectrum with DFT/6-31G*(d,p)-B3LYP level in vacuum were performed. This method was used to compute the 156 singlet → singlet transitions in vacuum (Fig. 1).

From an inspection to the frontier molecular orbitals of **3a** (Fig. 2) it is seen that the HOMO−1 is localized on the substitute triazole of mixed σ- and π-character (C(14) and C(15) atoms), both of π and partially π^*-characters of C- and N-atoms, C(19)/C(20), C(17)/N(18) atoms, and nb on the N (16)/O atoms.

The HOMO is also localized on the substitute triazole of mixed σ- and π-characters of oxygen O, C(7) and C(13) atoms, π and partially π^*-characters on the N(9)/C(8), C(11)/N(12) and N(10)/C(11) atoms. The LUMO is of antibonding character with π^*-symmetry localized on the aromatic rings C(2)/C(3) C(5)/C(6), C(1) and C(4), and on the C(7), C(8) atoms, respectively. Similarly, LUMO + 1 is of π^* orbital of C(1)/C(6), C(3)/C(4), C(2) and C(5) atoms, and on the C(7), C(8) atoms, respectively. LUMO + 2 is mostly of π^* orbital combination of N(18)/C(19) bond, N(16), C(17) and C(20) atoms, and on C(14) and C(15) atoms.

Considering that the spectrum of **3a** exhibits intense absorption bands in the about 324–236 nm range some additional intraligand transitions are expected at higher energies in the calculation. The assignment of calculated transitions to the experimental bands is based on the excitation energy and oscillator strength of the calculated transitions. The results are shown in Fig. 2 and Table 2, where selected transitions, with significant oscillator strength, are listed. The HOMO–LUMO gap is a typical quantity to describe the dynamic stability of any molecule. The HOMO–LUMO gap of **3a** (HOMO = −6.311 eV, LUMO = −3.289 eV and The HOMO–LUMO gap is 3.022 eV) is quite a sufficient level for electron transitions. Therefore, the lowest energy absorption is assigned as the $\pi \rightarrow \pi^*$ charge transfer [57] (Fig. 3).

4.5. Crystal structures determination of *3a, 3b* and *3c*

Crystallographic data of the compound **3a** is shown in Table 3. Molecular system exhibit weak C—H...N and C—H...O type

Table 4
Hydrogen-bond geometry (Å, °) of compounds **3a–c.**

3a	D–H...A	D–H	H...A	D...A	D–H...A
	C1—H1... N3	0.93	2.09	2.880(3)	142.4
	C2—H2... O1	0.93	2.44	3.246(3)	144.3
	C24—H24B... O1	0.97	2.49	3.382(4)	152
3b	D—H...A	D–H	H...A	D...A	D–H...A
	N3—H22...O3	0.919(15)	1.882(16)	2.7976(15)	174.7(13)
	C9—H9B...O3	0.980(16)	2.533(16)	3.4934(19)	166.3(12)
3c	D—H...A	D–H	H...A	D...A	D–H...A
	N3—H33...N6	0.91(2)	1.98(2)	2.8894(17)	172.8(17)
	C2—H2...O2A	0.93(3)	2.46(3)	3.300(12)	150(2)
	C7—H7A...O3	0.970(18)	2.431(19)	3.390(2)	170.3(14)
	C10—H10B...O3	0.960(16)	2.525(16)	3.3997(18)	151.6(12)
	C15—H15...O1A	0.959(17)	2.60(2)	3.486(13)	154.4(15)

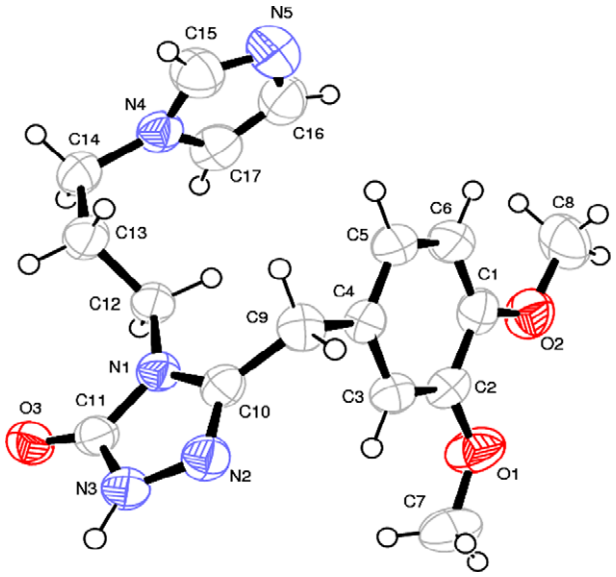

Fig. 5. Ortep III diagram of **3b.**

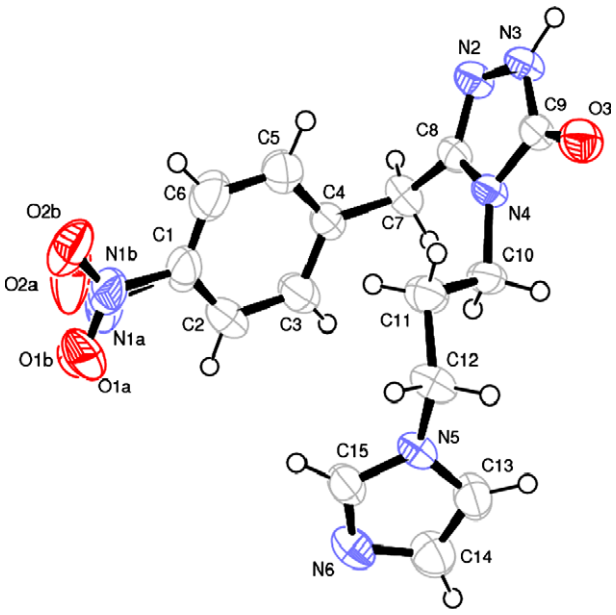

Fig. 7. Ortep III diagram of **3c**.

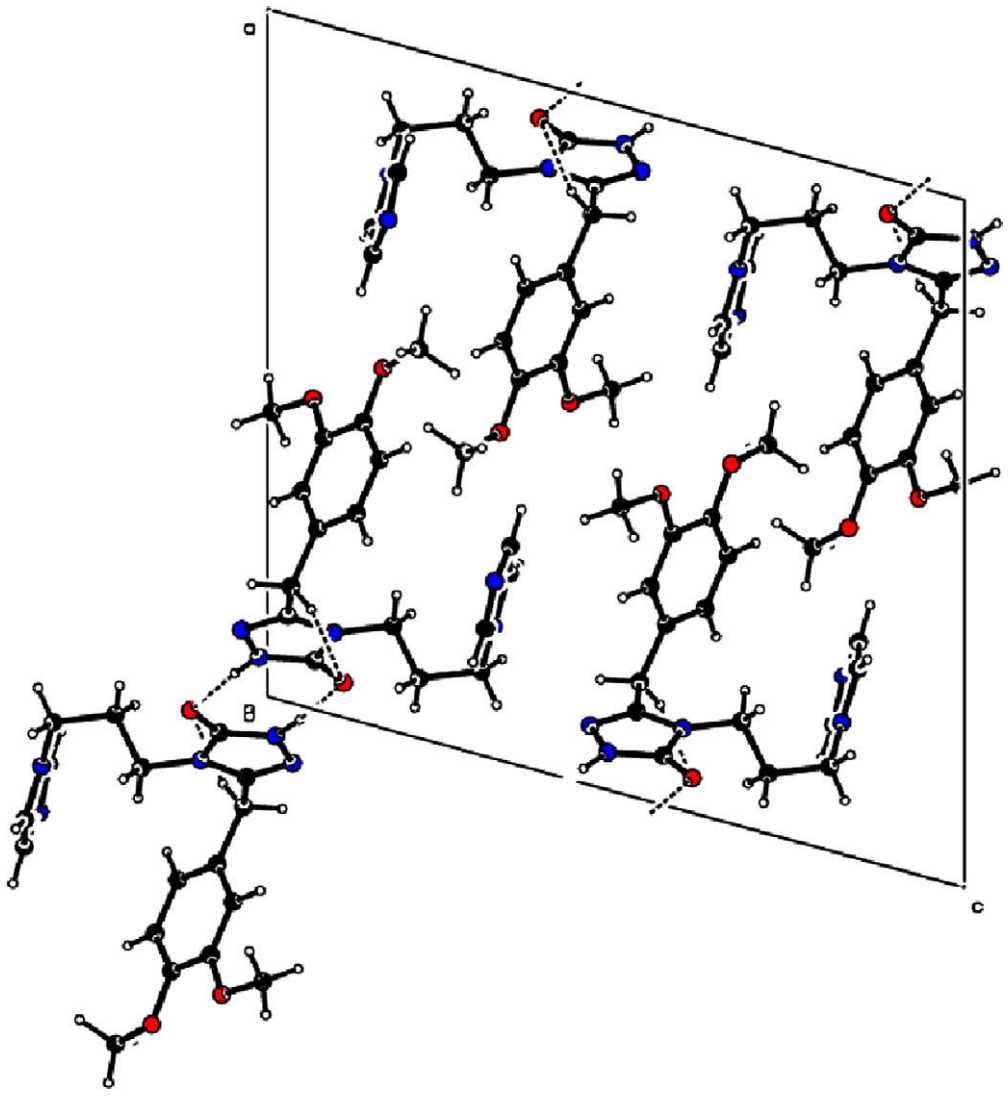

Fig. 6. Packing diagram of **3b** along the b axes.

intermolecular interactions, namely C1—H1...N3, C2—H2...O1 and C24—H24B...O1, resulting in an intricate three-dimensional network. The adjacent O1 atom, attached to the triazole ring, at (x, y, z) acts as a hydrogen bond acceptor to atom C1 at ($x+1$, y, z) and C2 at ($x+1/2$, $-y+3/2$, z) forming rings with graph set R_2^1 [58] shown in Fig. 4. There is also stacking interaction between C13-H13B...Cg(2), where Cg(2) is plane N4/C2/C1/N5/C4, the distance H...Cg is 2.84 Å and the angle X—H...Cg is 163°, with the symmetry code ($1-x$, $1-y$, $1/2+z$), the details of the H-bond is shown in Table 4 (Fig. 5).Crystallographic data of the compound **3b** is shown in Table 3. The compound **3b** is not planar like as **3a**. The dihedral angle between the triazole ring (C10/C11/N1/N2/N3) and the phenyl ring (C1/C2/C3/C4/C5/C6) is 89.33(5)° showing that these systems are perfect perpendicular to each other. Although the title compound has no classical hydrogen bond, it does exhibit weak N—H...O and C—H...O type hydrogen bonds are found in crystal packing, namely N3—H22...O3 (symmetry code: $-x,-y+1$, $-z+1$) and C9—H9...O3 (symmetry code: x, $y-1$, z) where adjacent atom O3 accepts hydrogen bonds from C—H donors (Table 4, Fig. 6). There is also π–π stacking interaction in the title compound, **3b**. The perpendicular distance between the Cg1 ring in a neighboring molecule is 3.49 Å at ($-x$, $1-y$, $-z$) [Cg1 is the ring centroid of the N1—C11 ring]. Both compounds **3a** and **3b** exhibit weak, but slightly different, intermolecular attractions. In **3a** C1—H1...N3, C2—H2...O1, C24—H24B...O1 and C—H...π interactions, while in **3b**, the interactions are N3—H22...O3, C9—H9...O3 and π–π.

Crystallographic data of the compound **3c** is shown in Table 3. The high values of the displacement parameters of the N and O atoms of the nitro group attached the phenyl indicating disorder of this group. Following sequence of the refinement and difference Fourier syntheses, disordered atoms, N1, O1 and O2 was recognized in 52(2):48(2) ratio in the nitro group. Their atomic displacement parameters are slightly larger than those of the other atoms.

In the compound **3c**, the ring systems are almost planar whereas the whole molecule is not planar (Fig. 7). The dihedral angle between the phenyl and triazole ring system is 89.94(5)°, that shows these systems are perpendicular to the each other. The

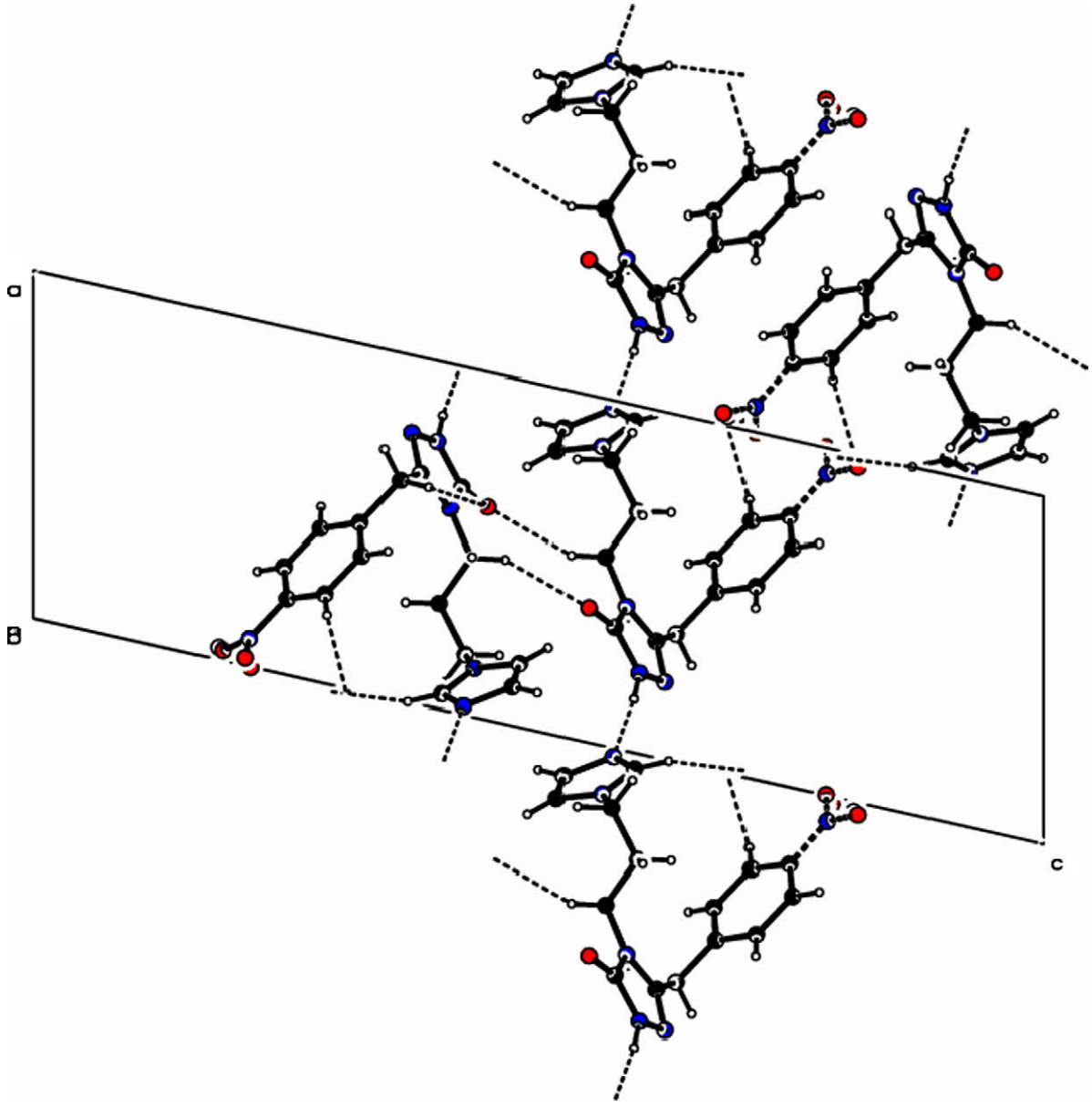

Fig. 8. Packing diagram of **3c** along the b axes.

molecular geometry of the triazole ring is in agreement values with the structures 3-[(5-Methyl-2-oxo-1,3-benzoxazol-3-yl)methyl]-4-phenyl-1H-1,2,4-triazole-5(4H)-thione [59] and 4-Allyl-3-[(5-methyl-2-oxo-1,3-benzoxazol-3-yl)methyl]-1H-1,2,4-triazole-5(4H)-thione [60].

The molecular structure is stabilized by N—H...N and C—H...O type intermolecular hydrogen bonds. In the compound **3c**, the adjacent O atom of the triazole ring acts as a hydrogen bond acceptor involving an intermolecular interaction with atom C7 and atom C10, like as the molecules **3a** and **3b**. Namely, C7-H7A...O3 (symmetry code: x, $y-1$, z), C10—H10B...O3 (symmetry code: $-x+1$, $-y+2$, $-z+1$). The latter interaction link the molecules into one-dimensional chain along (1 0 0) (Fig. 8), these interactions are, N3—H33...N6 (symmetry code: $x-1$, $y+1$, z), C2—H2...O2A (symmetry code: $-x+2$, $y-1/2$, $-z+3/2$) and C15—H15...O1A (symmetry code: $-x+2$, $y+1/2$, $-z+3/2$). The details of the hydrogen bonds are shown in the Table 4. There is also weak π–π interaction between the Cg2 ring in a neighboring molecule is 3.97 Å at ($2-x$, $2-y$, $-z$) [Cg2 is the ring centroid of the N5—C15 ring].

5. Conclusions

In conclusion, new triazole-3-one derivatives containing an imidazol ring, which are fundamental compounds in the preparation of ionic liquids and used as a antimicrobial substance, have been prepared and characterized by combination of X-ray crystallography, elemental analysis, ^{1}H- and ^{13}C NMR spectra, mass spectra, IR and UV–vis spectra, and theoretical methods. In the compound **3a**, all the ring systems are completely planar, while the complete molecule is non-planar. In addition, while oxygen, nitrogen (2, 3 and 5) atoms are lie out of rings, especially aliphatic C(23) atom is twisted into cavity of molecule. We have, however attempted to assign the calculated frequencies to the corresponding observed values based on the concept of group frequencies and intensity profiles. The compound **3b**, $C_{17}H_{21}N_5O_3$, is not planar. In the compound **3c**, $C_{15}H_{16}N_6O_3$, the ring systems are almost planar whereas the whole molecule is not planar.

Acknowledgements

This study was supported by Grants from Karadeniz Technical University (project No.: 2007.111.002.11) and the scientific and technological research council (TUBITAK project No.: 107T065) of Turkey.

References

[1] T. Tsukuda, Y. Shiratori, M. Watanabe, H. Ontsuka, K. Hattori, M. Shirai, N. Shimma, Bioorg. Med. Chem. Lett. 8 (1998) 1819.
[2] İ. Küçükgüzel, Ş.G. Küçükgüzel, S. Rollas, G. Ötük-Sanış, O. Özdemir, İ. Bayrak, T. Altuğ, J.P. Staples, Il Farmaco 59 (2004) 893.
[3] B. Modzelewska, J. Kalabun, Pharmazie 54 (1999) 503.
[4] B.S. Holla, K.N. Poorjary, B.S. Rao, M.K. Shivananda, Eur. J. Med. Chem. 37 (2002) 511.
[5] E. Palaska, G. Sahin, P. Kelicen, N.T. Durlu, G. Altınok, Il Farmaco 57 (2002) 101.
[6] S. Tehranchian, T. Akbarzadeh, M.R. Fazeli, H. Jamalifar, A. Shafiee, Bioorg. Med. Chem. Lett. 15 (2005) 1023.
[7] (a) M.I. Husain, M. Amir, J. Indian Chem. Soc. 63 (1986) 317;
(b) M.I. Husain, M. Amir, Chem. Abstr. 106 (1987) 176272h.
[8] S.H.L. Chiu, S.E.W. Huskey, Drug Metabol. Dispos. 26 (1998) 838.
[9] R. Eliott, R.L. Sunley, D.A. Griffin, Chem. Abstr. 107 (1987) 134310n.
[10] P.E. Goss, K. Strasser-Weippl, Best Pract. Res. Clin. End. Met. 18 (2004) 113.
[11] J.R. Santen, Steroids 68 (2003) 559.
[12] M. Clemons, R.E. Colemon, S. Verma, Cancer Treat. Rew. 30 (2004) 325.
[13] S. Chen, Y.C. Kao, C.A. Laughton, J. Steroid Biochem. 61 (1997) 107.
[14] J.S. Wilkes, M.J. Zaworotko, J. Chem. Soc. Chem. Commun. (1992) 965.
[15] J. Fuller, R.T. Carlin, H.C. De Long, D. Haworth, J. Chem. Soc., Chem. Commun. (1994) 299.
[16] P. Bonhote, A.-P. Dias, M. Armand, N. Papageorgiou, K. Kalyanasundaram, M. Gratzel, Inorg. Chem. 35 (1996) 1168.
[17] (a) D.R. MacFarlane, P. Meakin, J. Sun, N. Amini, M. Forsyth, J. Phys. Chem. B 103 (1999) 4164;
(b) D.R. MacFarlane, J. Huang, M. Forsyth, Nature 402 (1999) 792.
[18] R. Hagiwara, T. Hirashige, T. Tsuda, Y. Ito, J. Fluorine Chem. 99 (1999) 1.
[19] H. Matsumoto, T. Matsuda, Y. Miyazaki, Chem. Lett. (2000) 1430.
[20] (a) H. Matsumoto, M. Yanagida, K. Tanimoto, M. Nomura, Y. Kitagawa, Y. Miyazaki, Chem. Lett. (2000) 922;
(b) H. Matsumoto, H. Kageyama, Y. Miyazaki, Chem. Lett. (2001) 182.
[21] H. Ohno, K. Ito, Chem. Lett. (1998) 751.
[22] M. Yoshizawa, H. Ohno, Chem. Lett. (1999) 889.
[23] S.I. Lall, D. Mancheno, S. Castro, V. Behaj, J.I. Cohen, R. Engel, Chem. Commun. (2000) 2413.
[24] J.H. Davis Jr., K.J. Forrester, T. Merrigan, Tetrahedron Lett. 39 (1998) 55.
[25] A.S. Larsen, J.D. Holbrey, F.S. Tham, C.A. Reed, J. Am. Chem. Soc. 122 (2000) 7264.
[26] For reviews, see: (a) J.S. Wilkes, Green Chem. 4 (2002) 73;
(b) R. Sheldon, Green Chem. 4 (2002) 73;
(c) P. Wasserscheid, W.K. Angew, Chem, Int. Ed. 39 (2000) 3772;
(d) Y. Chauvin, .H. Olivier, Chemtech (1995) 26.
[27] V.R. Koch, C. Nanjundiah, G.B. Appetecchi, B. Scrosati, J. Electrochem. Soc. (1995) L116.
[28] A.B. McEwen, H.L. Ngo, K. LeCompte, J.L. Goldman, J. Electrochem. Soc. 146 (1999) 1687.
[29] A. Noda, M. Watanabe, Electrochim. Acta 45 (2000) 1265.
[30] (a) N. Papageorgiou, Y. Athanassov, M. Armand, P. Bonhô te, H. Pettersson, A. Azam, M. Gratzel, J. Electrochem. Soc. 143 (1996) 3099;;
(b) H. Matsumoto, T. Matsuda, T. Tsuda, R. Hagiwara, Y. Ito, Y. Miyazaki, Chem. Lett. (2001) 26.
[31] M. Doyle, S.K. Choi, G. Proulx, J. Electrochem. Soc. 147 (2000) 34.
[32] T. Welton, Chem. Rev. (1999) 2071.
[33] (a) J.G. Huddleston, H.D. Willauer, R.P. Swatloski, A.E. Visser, R.D. Rogers, Chem. Commun. (1998) 1765;
(b) A.E. Visser, R.P. Swatloski, W.M. Reichert, R. Mayton, S. Sheff, A. Wierzbicki, J.H. Davis Jr., R.D. Rogers, Chem. Commun. (2001) 135.
[34] V.V. Nomboodiri, R.S. Varma, Org. Lett. (2002) 3161.
[35] Recent examples: (a) Y. Gu, F. Shi, Y. Deng, J. Org. Chem. 69 (2004) 391;
(b) F. Shi, H. Xion, Y. Gu, S. Guo, Y. Deng, Chem. Commun. (2003) 1054;
(c) E.J. Kim, S.Y. Ko, C.E. Song, Helv. Chim. Acta 86 (2003) 894;
(d) J.N. Rosa, C.A.M. Afonso, A.G. Santos, Tetrahedron 57 (2001) 4189;
(e) T. Tsuchimoto, T. Maeda, E. Shirakawa, Y. Kawakami, Chem. Commun. (2000) 1573;
(f) C.E. Song, W.H. Shim, E.J. Roh, S.-G. Lee, J.H. Choi, Chem. Commun. 2 (2001) 1122.
[36] R. Hagiwara, Y.J. Ito, J. Fluorine Chem. 105 (2000) 221.
[37] J.D. Holbrey, K.R. Seddon, J. Chem. Soc., Dalton Trans. (1999) 2133.
[38] Stoe & Cie (2002). X-AREA (Version 1.18) and X-RED32 (Version 1.04). Stoe & Cie, Darmstadt, Germany.
[39] G.M. Sheldrick, SHELXS97 and SHELXL97, University of Göttingen, Germany, 1997.
[40] Burnett M.N., Johnson C.K. (1996). ORTEPIII. Report ORNL-6895. Oak Ridge National Laboratory, Tennessee, USA.
[41] L.J. Farrugia, J. Appl. Cryst. 32 (1999) 837.
[42] M. Nardelli, J. Appl. Cryst. 28 (1995) 659.
[43] A. Ikizler, K. Sancak, Rov. Roumaine Chim. 43 (1998) 133.
[44] R. Milcent, C. Redeuilh, J. Heterocycl. Chem. 16 (1979) 403.
[45] G. Laus, V. Kahlenberg, D.M. Többens, R.K.R. Jetti, U.J. Griesser, J. Schütz, E. Kristeva, K. Wurst, H. Schottenberger, Crystal Growth & Desing 6 (2006) 404.
[46] C. Aleman, J. Puiggali, J. Org. Chem. 64 (1999) 351.
[47] M. Er, K. Sancak, I. Değirmencioğlu, K. Serbest, J. Mol. Struct. 882 (2008) 35–46.
[48] M.J. Frisch, G.W. Trucks, H.B. Schlegel, G.E. Scuseria, M.A. Robb, J.R. Cheeseman, J.A. Montgomery Jr., T. Vreven, K.N. Kudin, J.C. Burant, J.M. Millam, S.S. Iyengar, J. Tomasi, V. Barone, B. Mennucci, M. Cossi, G. Scalmani, N. Rega, G.A. Petersson, H. Nakatsuji, M. Hada, M. Ehara, K. Toyota, R. Fukuda, J. Hasegawa, M. Ishida, T. Akajima, Y. Honda, O. Kitao, H. Nakai, M. Klene, X. Li, J.E. Knox, H.P. Hratchian, J.B. Cross, C. Adamo, J. Jaramillo, R. Gomperts, R.E. Stratmann, O. Yazyev, A.J. Austin, R. Cammi, C. Pomelli, J.W. Ochterski, P.Y. Ayala, K. Morokuma, G.A. Voth, P. Salvador, J.J. Dannenberg, V.G. Zakrzewski, S. Dapprich, A.D. Daniels, M.C. Strain, O. Farkas, D.K. Malick, A.D. Rabuck, K. Raghavachari, J.B. Foresman, J.V. Ortiz, Q. Cui, A.G. Baboul, S. Clifford, J. Cioslowski, B.B. Stefanov, G. Liu, A. Liashenko, P. Piskorz, I. Komaromi, R.L. Martin, D.J. Fox, T. Keith, M.A. Al-Laham, C.Y. Peng, A. Nanayakkara, M. Challacombe, P.M.W. Gill, B. Johnson, W. Chen, M.W. Wong, C. Gonzalez, J.A. Pople, GAUSSIAN-03, Revision C.02, Gaussian, Inc., Pittsburgh, PA, (2003).
[49] K. Sancak, M. Er, Y. Ünver, M. Yildirim, I. Degirmencioglu, K. Serbest, Trans. Met. Chem. 32 (2007) 16.
[50] J.B. Foresman, E. Frisch, Exploring Chemistry with Electronic Structure Methods: A Guide to Using Gaussian, Gaussian, Pittsburg, PA, 1993.
[51] A.P. Scott, L. Radom, J. Phys. Chem. 100 (41) (1996) 16502.
[52] G.W. Burton, T. Doba, E.J. Gabe, L. Hughes, F.L. Lee, L. Prasad, K.U. Ingold, J. Am. Chem. Soc. 107 (1985) 7053.
[53] G.W. Burton, Y. Le Page, E.J. Gabe, K.U. Ingold, J. Am. Chem. Soc. 102 (1980) 7791.
[54] G.W. Burton, K.U. Ingold, J. Am. Chem. Soc. 103 (1981) 6472.
[55] M. Silverstein, G. Clayton Basseler, C. Morill, Spectrometric Identification of Organic Compounds, Wiley, New York, 1981.
[56] H. Aslan, U. Flörke, N. Külcü, Spectrochim. Acta A 67 (2007) 936.

[57] A.H. Jubert, M.L. Alegre, R.P. Diez, A.B. Pomilio, V.D. Szewczuk, Spectrochimica Acta Part A 66 (2007) 1208.
[58] J. Bernstein, R.E. Davies, L. Shimoni, N.L. Chang, Angew. Chem. Int. Ed. Engl. 34 (1995) 1555.
[59] Y. Köysal, Ş. Işık, U. Salgın, N. Gökhan, Acta Cryst. Section E 63 (2007) 2462.
[60] Y. Köysal, Ş. Işık, U. Salgın, N. Gökhan, Acta Cryst. Section E 63 (2007) 2463.